

AD-A113 913

PACIFIC-SIERRA RESEARCH CORP SANTA MONICA CA

F/G 20/14

A NUMERICAL METHOD FOR USING A RAY TRACING PROGRAM TO COMPUTE R--ETC(U)

MAR 82 R E WARREN, R N DEWITT, C R WARBER

F19628-80-C-0065

UNCLASSIFIED

PSR-1121

RADC-TR-82-45

NL

| OF |
AD A
113913



END
DATE
FILMED
05-82
DTIC

A
39

12

RADC-TR-82-45
Final Technical Report
March 1982



A NUMERICAL METHOD FOR USING A RAY TRACING PROGRAM TO COMPUTE RADIO FIELDS IN REGIONS OF STRONG FOCUSING

Pacific-Sierra Corporation

**R. E. Warren
R. N. DeWitt
C. R. Warber**

APPROVED FOR PUBLIC RELEASE; DISTRIBUTION UNLIMITED

AL A113913

DTIC FILE COPY

**ROME AIR DEVELOPMENT CENTER
Air Force Systems Command
Griffiss Air Force Base, New York 13441**

DTIC
EXCERPTS
APR 28 1982
D
H

82 04 27 108

This report has been reviewed by the RADC Public Affairs Office (PA) and is releasable to the National Technical Information Service (NTIS). At NTIS it will be releasable to the general public, including foreign nations.

RADC-TR-82-45 has been reviewed and is approved for publication.

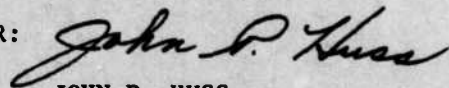
APPROVED:


PAUL A. KOSSEY
Project Engineer

APPROVED:


ALLAN C. SCHELL, Chief
Electromagnetic Sciences Division

FOR THE COMMANDER:


JOHN P. HUSS
Acting Chief, Plans Office

If your address has changed or if you wish to be removed from the RADC mailing list, or if the addressee is no longer employed by your organization, please notify RADC (EEPL), Hanscom AFB MA 01731. This will assist us in maintaining a current mailing list.

Do not return copies of this report unless contractual obligations or notices on a specific document requires that it be returned.

UNCLASSIFIED

SECURITY CLASSIFICATION OF THIS PAGE (When Data Entered)

REPORT DOCUMENTATION PAGE		READ INSTRUCTIONS BEFORE COMPLETING FORM
1. REPORT NUMBER RADC-TR-82-45	2. GOVT ACCESSION NO. AD-A113 913	3. RECIPIENT'S CATALOG NUMBER
4. TITLE (and Subtitle) A NUMERICAL METHOD FOR USING A RAY TRACING PROGRAM TO COMPUTE RADIO FIELDS IN REGIONS OF STRONG FOCUSING	5. TYPE OF REPORT & PERIOD COVERED Final Technical Report Apr 80 - Jun 81	
	6. PERFORMING ORG. REPORT NUMBER PSR Report 1121	
7. AUTHOR(s) R. E. Warren R. N. DeWitt C. R. Warber	8. CONTRACT OR GRANT NUMBER(s) F19628-80-C-0065	
9. PERFORMING ORGANIZATION NAME AND ADDRESS Pacific-Sierra Research Corporation 1456 Cloverfield Boulevard Santa Monica CA 90404	10. PROGRAM ELEMENT, PROJECT, TASK AREA & WORK UNIT NUMBERS 62702F 46001647	
11. CONTROLLING OFFICE NAME AND ADDRESS Deputy for Electronic Technology (RADC/EEPL) Hanscom AFB MA 01731	12. REPORT DATE March 1982	
	13. NUMBER OF PAGES 58	
14. MONITORING AGENCY NAME & ADDRESS (if different from Controlling Office) Same	15. SECURITY CLASS. (of this report) UNCLASSIFIED	
	15a. DECLASSIFICATION/DOWNGRADING SCHEDULE N/A	
16. DISTRIBUTION STATEMENT (of this Report) Approved for public release; distribution unlimited.		
17. DISTRIBUTION STATEMENT (of the abstract entered in Block 20, if different from Report) Same		
18. SUPPLEMENTARY NOTES RADC Project Engineer: Paul A. Kossey (EEPL)		
19. KEY WORDS (Continue on reverse side if necessary and identify by block number) Caustics Radio Propagation Ray Tracing		
20. ABSTRACT (Continue on reverse side if necessary and identify by block number) This paper presents a practical method of computing radio fields in regions of strong focusing, using ray intercept data provided by a standard ray tracing program. The procedure extends the usefulness of the ray trace by allowing fields to be computed near caustics and cusps where ray density calculations fail. Using a plane wave decomposition of the field components, phase integrals are computed by curve fitting intercepts of ray traced through ionospheric or tropospheric media whose refractive in-		

DD FORM 1 JAN 73 1473 EDITION OF 1 NOV 65 IS OBSOLETE

UNCLASSIFIED

SECURITY CLASSIFICATION OF THIS PAGE (When Data Entered)

UNCLASSIFIED

SECURITY CLASSIFICATION OF THIS PAGE(When Data Entered)

← dices vary arbitrarily with altitude. A numerical algorithm is described for performing the plane-wave angular spectral integrations. This procedure avoids the complications associated with higher order asymptotic techniques, allowing a much broader range of refractivity-index profiles to be analyzed by a single method. It is applied to two sample profiles, and the results agree very closely with higher order stationary-phase estimates in caustic regions. Moreover, the computer code runs efficiently, despite the presence of highly oscillatory integrands. The method is capable of including the effects of weak collisions, the spherical earth, and azimuthally dependent transmitter configurations. An extension of the angular spectral representations is given to include regions throughout the vicinity of a thin, overdense layer.

A

UNCLASSIFIED

SECURITY CLASSIFICATION OF THIS PAGE(When Data Entered)

CONTENTS

FIGURES v

PREFACE vii

Section

I. INTRODUCTION 1

II. UNIFORM ANGULAR SPECTRAL REPRESENTATION 4

III. COMPUTATION OF PHASE FROM RAY TRACE DATA 8

IV. NUMERICAL EXAMPLES 14

 Linear Ionospheric Profile 14

 Hyperbolic Secant Profile with Collisions 17

V. UNIFORM ANGULAR SPECTRAL REPRESENTATION FOR
 AN EVANESCENT LAYER 22

 Asymptotic Limits 27

 Numerical Example 30

VI. CONCLUSIONS 33

REFERENCES 35

Appendix

A. CURVE FITTING THE RAY INTERCEPT DATA 39

B. PLP ALGORITHM 43

SYMBOLS 45



Accession For	
NTIS GRA&I	<input checked="" type="checkbox"/>
DTIC TAB	<input type="checkbox"/>
Unannounced	<input type="checkbox"/>
Justification	
By _____	
Distribution/	
Availability Codes	
Dist	Avail and/or Special
A	

FIGURES

1. Ray intercepts on horizontal planes at various heights z for the linear ionospheric model (27), with $h = 100$ km, $\alpha = 0.002$ km ⁻¹	15
2. Range dependence of the electric field modulus at the ground for the linear ionospheric model (27), with $h = 100$ km, $\alpha = 0.002$ km ⁻¹	18
3. Ray intercepts on horizontal planes at various heights z for the sech ionospheric model (30), with $a = 0.9$, $\alpha = 0.05$ km ⁻¹ , $z_m = 100$ km, $Z = 0$	19
4. Range dependence of the electric field modulus at a height z of 88 km for the linear ionospheric model $n^2 = 1 - a^2 \operatorname{sech}^2 [\alpha(z - z_m)]$, with $a = 0.9$, $\alpha = 0.05$ km ⁻¹ , $z_m = 100$ km	21
5. Transmission through the sech ionospheric layer, Eq. (30), at various values of the parameter $a = f/f_p$	32

PREFACE

This report summarizes Pacific-Sierra Research Corporation's (PSR) work in developing a practical numerical method for computing radio field strengths in regions of strong focusing, using input from a standard ray tracing program. The computer program was designed for use with the Jones-Stephenson high-frequency ray trace code.

PRECEDING PAGE BLANK-NOT FILMED

I. INTRODUCTION

This report presents a method for using ray tracing to calculate radio field strengths in strong-focusing regions of the ionosphere or troposphere. Ray tracing is an established technique for predicting radio field strengths in regions without strong focusing. Because of the versatility and numerical efficiency of ray tracing, it is a desirable technique for computing radio fields in strong-focusing regions, using a state-of-the-art ray tracing program such as that of *Jones and Stephenson* [1975]. This report presents a practical numerical method for doing so.

The procedure for computing radio fields in stratified media from ray tracing outside caustic regions uses the well-known correspondence--developed by *Booker* [1939], *Budden* [1961a], and others--between ray trajectories and the first-order asymptotic approximation to the angular spectral representation of the field components. *Budden* [1976] and others show how the phase and amplitude of fields are directly related to the path-integrated refractive-index variation and the ray curvature, both easily computed with a ray tracing program in regions where neighboring rays do not cross. That correspondence solves the radio field problem for stratified media outside caustic areas.

Breakdown of the first-order stationary-phase result near caustics has led to the development of higher order asymptotic formulas that uniformly interpolate the field through caustic regions and can extend field strength calculations based on ray density into strong focusing regions [*Maslin*, 1976b; *Budden*, 1976]. Unfortunately, asymptotic

methods have two drawbacks that make them inconvenient for use with a ray tracing program:

1. Different closed-form expressions involving special functions are needed for different degrees of focusing--e.g., Airy functions for caustics and *Pearcey's* [1946] function for cusps. Further, only the Airy functions are both well known and convenient for numerical calculation.
2. The contributions from all rays intercepting each field point must be calculated--a numerically cumbersome procedure requiring a search to identify the specific plane wave components intercepting a given field point.

Because of these limitations, only simple refractive-index profiles can be studied, wasting much of the potential power of the ray trace.

An alternative to asymptotic methods is to evaluate the integral expressions for the field numerically using phase information derived from the ray trace. Thus, a broader range of refractive-index profiles could be analyzed by a single method; cusps and even higher order focusing effects would require no special analysis. However, this method has two potential difficulties:

1. The integrands are highly oscillatory and standard numerical integration techniques fail.
2. For points in the vicinity of caustics, more accurate phase differences between neighboring plane-wave spectral components are needed than the ray trace can supply directly through its path integration of the refractive-index variation. That limitation is simply due to a loss of numerical

precision and disappears if the ray directions through a given field point are widely separated--as indeed they are when the first-order calculation is valid.

The numerical method presented here overcomes these difficulties.

Section II briefly summarizes the plane-wave angular spectral representation of radio fields, including *Budden's* [1976] generalization to allow the phase integral method to be applied uniformly throughout reflection regions. Section III discusses a method for using ray trace data to accurately estimate the phase differences between neighboring plane-wave components. Section IV shows that the highly oscillatory spectral integrations can be performed by a numerical quadrature technique developed independently by *Woodie* [1976] and *Barakat* [1976]. Field calculations using our method are compared with asymptotic results of *Maslin* [1976b].

The only potentially important feature lost with our approach is the ability to include evanescent wave components in the spectral integral; they must be excluded if the ray trace can propagate only real rays. That limitation precludes treating problems such as leakage through layers at frequencies slightly below the penetration frequency. Section V gives a partial solution to the leakage problem, generalizing *Budden's* single-reflection height interpolation to the case of two arbitrarily close roots of the *Booker* q function.

For convenience, mathematical details of the phase determination and numerical integration procedures are given in two appendixes. Throughout our analysis, we assume an isotropic propagation medium varying in only one dimension--which, however, can be either height (flat earth) or radius (spherical earth).

II. UNIFORM ANGULAR SPECTRAL REPRESENTATION

The basis of our analysis is *Budden's* [1976] integral expression for a field component F that is uniformly valid throughout caustic and reflection regions:

$$F(x, y, z) = \iint dS_1 dS_2 G(S_1, S_2) (C/q)^{1/2} 2\xi^{1/4} \pi^{1/2} \text{Ai}(\xi) \times \exp \left[-ik \left(S_1 x + S_2 y + \int_0^{z_0} dzq \right) \right], \quad (1)$$

written as a superposition, weighted by the function G , of plane waves with complex direction cosines S_1, S_2, C in free space. We use Cartesian coordinates x, y, z , with z denoting altitude; k is the free-space wave number. The function q is defined as

$$q^2 = n^2(z) - S_1^2 - S_2^2, \quad (2)$$

where the complex refractive index n is taken to be a function of height z only. Following *Budden*, ξ is defined as

$$\xi = \left(\frac{3}{2} ik \int_{z_0}^z dzq \right)^{2/3}, \quad (3)$$

Ai is Airy's integral, and $z_0(S_1, S_2)$ is the reflection height [$q(z_0) = 0$] for the plane wave component labeled S_1, S_2 . *Budden* [1976] provides the proper integration contour and phase choices

that make (1) unambiguous. When $|\xi| \gg 1$, the factor

$$2\xi^{1/4} \pi^{1/2} \text{Ai}(\xi) \exp\left(-ik \int_0^{z_0} dzq\right) \quad (4)$$

assumes the asymptotic form

$$\exp\left(-ik \int_0^z dzq\right) + i \exp\left(-ik \oint_0^z dzq\right), \quad (5)$$

representing a sum of upgoing and downgoing waves. The path integral over q in the second term is understood to circle the reflection height z_0 clockwise in the analytical continuation of height; on the downgoing path, q is chosen negative. Although it is valid to replace the Airy function factor (4) with the asymptotic limit (5) even at caustics when $|\xi| \gg 1$ [Maslin, 1976a], the Airy form is capable of including plane wave components near a reflection level, where $q(S_1, S_2)$ vanishes. For completeness we prefer to retain the general form (1) although, for most spectral components appearing in the integral, the asymptotic approximation using (5) is both adequate and faster to compute. The asymptotic form is in fact the basis for the higher order asymptotic approximations of fields near caustics and cusps constructed by Maslin [1976b]. His results contain Airy functions only because of his use of the uniform asymptotic method of Chester *et al.* [1957].

The spectral weighting function G is determined by both the field component represented by F and the transmitter. For most applications, the angular spectral dependence of G will be fairly simple.

For example, the spectral weighting of the y-component of the electric field in the magnetic dipole example studied by *MasLin* [1976b] and *Budden* [1976] is represented by

$$G(S_1, S_2) = G_0 S_1/C . \quad (6)$$

It is thus convenient to expand G in harmonics of its azimuthal dependence and treat each component separately. That is, we expand G as

$$G(S_1, S_2) = \sum_{n=-\infty}^{\infty} g_n(S) e^{in\phi} , \quad (7)$$

where

$$g_n(S) = \frac{1}{2\pi} \int_0^{2\pi} d\phi G(S_1, S_2) e^{-in\phi} , \quad (8)$$

and $S_1 = S \cos \phi$, $S_2 = S \sin \phi$. Substituting (7) into (1) and integrating over ϕ produces

$$F(x, y, z) = 2\pi \sum_{n=-\infty}^{\infty} i^n e^{in\psi} \int_0^{\infty} dS S g_n(S) (C/q)^{1/2} \Lambda(S, z) J_n(kS\rho) , \quad (9)$$

where $x = \rho \cos \psi$, $y = \rho \sin \psi$, and $\Lambda(S, z)$ denotes either the Airy function factor (4) or its asymptotic approximation (5). For points not directly over the transmitter, the Bessel functions may be approximated as

$$J_n(kS\rho) \approx \left(\frac{2}{\pi kS\rho}\right)^{1/2} \cos\left(kS\rho - n\frac{\pi}{2} - \frac{\pi}{4}\right). \quad (10)$$

Specializing to the magnetic dipole represented by (6) for the plane $y = 0$, using (10) and the asymptotic form of Λ , yields

$$F(x, 0, z) \approx (2\pi/kx)^{1/2} e^{i\pi/4} G_0 \int_{-\infty}^{\infty} dS S^{3/2} (Cq)^{-1/2} \\ \times \exp\left[-ik\left(Sx + \int_0^z dzq\right)\right] \quad (11)$$

for the upgoing wave. An analogous expression results for the reflected wave. Equation (11) here is equivalent to Eq. (7) of *Maslin* [1976b] and Eq. (23) of *Budden* [1976].

III. COMPUTATION OF PHASE FROM RAY TRACE DATA

For sufficiently simple refractive-index profiles, the phase integrals such as

$$\int_0^z dzq(S_1, S_2, z)$$

needed in (9) are most simply computed with numerical or analytic methods. For complicated media, however, such evaluation becomes tedious--especially when ducting with multiple turning points is involved. On the other hand, ray tracing techniques have been found useful in producing field estimates through ray density calculations for quite general ionospheric or tropospheric models [Wong, 1958; Budden and Terry, 1971]. The principal disadvantage of ray density calculations is their breakdown in caustic regions. Nonetheless, the identification of rays with spectral wave components is the basis for a simple means of using the ray trace to estimate the phase integrals required in the Budden/Maslin theory discussed above.

The connection between ray tracing and phase integration can be established through the Hamiltonian formalism. The following are the canonical equations [Haselgrove and Haselgrove, 1960] for the ray trajectory specified by position x, y, z and direction cosines S_1, S_2, q , where $S_1^2 + S_2^2 + q^2 = n^2(z)$:

$$\frac{dx}{d\tau} = \frac{\partial H}{\partial S_1}, \quad \frac{dy}{d\tau} = \frac{\partial H}{\partial S_2}, \quad \frac{dz}{d\tau} = \frac{\partial H}{\partial q} \quad (12)$$

and

$$\frac{dS_1}{d\tau} = -\frac{\partial H}{\partial x}, \quad \frac{dS_2}{d\tau} = -\frac{\partial H}{\partial y}, \quad \frac{dq}{d\tau} = -\frac{\partial H}{\partial z}. \quad (13)$$

Here τ parameterizes the ray trajectory and can be taken to be the arc length along the ray. The Hamiltonian H can be specified in a number of ways; a convenient choice is

$$H = \frac{1}{2} \left[S_1^2 + S_2^2 + q^2 - n^2(z) \right] = 0. \quad (14)$$

The ray trajectory results from substituting (14) into (12) and (13), then solving them either numerically or analytically. Since S_1 and S_2 are conserved along the ray trajectory (Snell's law), the spectral component labeled S_1, S_2 can be identified with a unique ray. From elementary calculus

$$\frac{dx}{dz} = \frac{dx}{d\tau} \frac{d\tau}{dz} = \frac{\partial H}{\partial S_1} \frac{\partial H}{\partial q} = \frac{S_1}{q} \quad \text{and} \quad \frac{dy}{dz} = \frac{S_2}{q}, \quad (15)$$

and integration gives

$$x(S_1, S_2, z) = S_1 \int_0^z dzq^{-1} = -\frac{\partial}{\partial S_1} \int_0^z dzq(S_1, S_2, z), \quad (16a)$$

$$y(S_1, S_2, z) = S_2 \int_0^z dzq^{-1} = -\frac{\partial}{\partial S_2} \int_0^z dzq(S_1, S_2, z), \quad (16b)$$

where (14) was used for the last step. Equations (16) are identical to Eq. (5) of *Maslin* [1976b] and are the ray tracing equations of

Booker [1939]. *Maslin* and *Budden* derive them by applying the first-order stationary-phase method to the angular spectral representation (1). The important point is that (16) remain valid when the ray passes through a caustic, even though the associated first-order stationary-phase approximation to the field breaks down. Aside from a constant, the phase integral

$$\phi(S_1, S_2, z) = \int_0^z dzq(S_1, S_2, z)$$

is recovered by integrating (16) with respect to S_1 or S_2 . The integrands x or y are produced using ray intercepts on the plane at height z as a function of S_1, S_2 . Appendix A details this construction.

Because this method of constructing the phase from the ray trace uses the ray intercepts and not the path-integrated refractive-index variation directly, it provides a much more reliable estimate of the small phase differences between neighboring plane wave components. This is essential to the success of the approach.

Although ϕ is in general complex, only its real component can be recovered by this method, which employs a real-valued ray tracing program such as that of *Jones/Stephenson* [1975]. Thus, a primary assumption of our model is that evanescent waves contribute negligibly to the field represented by (9). Nevertheless, weak collisions may be included in this approach by formally tracing the rays as if they were real, then adding the path-integrated attenuation computed by the ray trace to the spectral weighting function G for each wave component [*Booker*, 1939].

The neglect of evanescent waves appears to be valid as long as the spectral weighting function G is continuous. For G continuous, the absence in the integral of spectral components with a slowly varying phase in the shadow region beyond the caustic leaves only rapidly varying components, leading to destructive interference and a decaying field. For an infinitely distant transmitter, however, there is only a single plane-wave component S_0 ; G thus becomes a delta function $\delta(S - S_0)$ and our model would not provide information about the field above the reflection height of the plane wave component S_0 .

Because q is double-valued, (16) can be taken to represent intercepts of either the upgoing or the reflected parts of the ray trajectory. In the latter case, the integral is understood to run up to z_0 , then to return to z with q changing sign as it passes through zero. Thus we define the phase of the up- and downgoing rays ϕ_u and ϕ_d as

$$\phi_u(S_1, S_2, z) = \int_0^z dzq(S_1, S_2, z) \quad (17)$$

and

$$\begin{aligned} \phi_d(S_1, S_2, z) &= \oint_0^z dzq(S_1, S_2, z) \\ &= \phi_u(S_1, S_2, z_0) + \int_{z_0}^z dzq . \end{aligned} \quad (18)$$

The ray trajectory is symmetrical about its reflection point, so (18) can be written

$$\phi_d(S_1, S_2, z) = \phi_u(S_1, S_2, z) + 2 \int_z^{z_0} dz |q| . \quad (19)$$

Integration of the up- and downgoing ray intercepts produces ϕ_u and ϕ_d on the plane at z only up to constants; the proper phase difference between the up- and downgoing waves is produced by requiring the phases to agree at the reflection point.

Substituting those results into (3), we obtain

$$\xi = \left[\frac{3}{4} ik(\phi_d - \phi_u) \right]^{2/3} , \quad (20)$$

and (9) becomes

$$F(x, y, z) = 2\pi \sum_{n=-\infty}^{\infty} i^n e^{in\psi} \int_0^1 dS S g_n(S) (C/q)^{1/2} 2\xi^{1/4} \pi^{1/2} \Lambda I(\xi) \\ \times \exp \left[-i \frac{k}{2} (\phi_d + \phi_u) \right] J_n(kS\rho) . \quad (21)$$

Using (10) for points not directly over the transmitter yields

$$F(x, y, z) \approx e^{i\pi/4} (2\pi/k\rho)^{1/2} \sum_{n=-\infty}^{\infty} e^{in\psi} \int_{-1}^1 dS g_n(S) \left(\frac{CS}{q} \right)^{1/2} \\ \times 2\pi^{1/2} \xi^{1/4} \Lambda I(\xi) \exp \left\{ -ik \left[S\rho + \frac{1}{2} (\phi_d + \phi_u) \right] \right\} . \quad (22)$$

In equations (21) and (22), the actual integration limits are determined by the rays that intercept the plane at z . For $|\xi| \gg 1$, the factor

$$2\pi^{1/2} \xi^{1/4} \Lambda i(\xi) \exp \left[-i \frac{k}{2} (\phi_d + \phi_u) \right] \quad (23)$$

becomes

$$\exp(-ik\phi_u) + i \exp(-ik\phi_d) . \quad (24)$$

In practice, *Budden and Terry* [1971] show $|\xi|$ need only be ≥ 1.3 to make (24) a good estimate of (23). Following *Budden* [1961], ξ is computed as

$$\xi = - \left| \frac{3}{4} k(\phi_d - \phi_u) \right|^{2/3} , \quad (25)$$

and

$$\xi^{1/4} = |\xi|^{1/4} e^{i\pi/4} . \quad (26)$$

These are the proper phase choices for producing the asymptotic form (24) from (23) well below the reflection height.

IV. NUMERICAL EXAMPLES

Although our method is suitable for a wide range of realistic profiles, we illustrate it by application to two relatively simple ionospheric profiles studied by *Maslin* [1976a,b], allowing our numerical results to be compared with his asymptotic results.

LINEAR IONOSPHERIC PROFILE

First consider the linear refractive-index height profile used by *Maslin* [1976a,b]:

$$\begin{aligned} n^2 &= 1, & z < h, \\ &= 1 - \alpha(z - h), & z > h, \end{aligned} \quad (27)$$

where α and h are constants. Because of the simplicity of the model, analytic expressions for the ray intercepts on an arbitrary horizontal plane at height z are easily found from (2) and (16); in the plane $y = 0$,

$$\begin{aligned} x(S) &= zS/C, & z < h \text{ upgoing}, \\ &= (2h + 4C^2/\alpha - z)S/C, & z < h \text{ downgoing}, \\ &= hS/C + \left[C - \sqrt{C^2 - \alpha(z - h)} \right] 2S/\alpha, & z > h \text{ upgoing}, \\ &= hS/C + \left[C + \sqrt{C^2 - \alpha(z - h)} \right] 2S/\alpha, & z > h \text{ downgoing}. \end{aligned} \quad (28)$$

Figure 1 plots $x(S)$ as a function of S for various heights z , using $h = 100 \text{ km}$, $\alpha = 0.002 \text{ km}^{-1}$. For graphical clarity, the intercepts

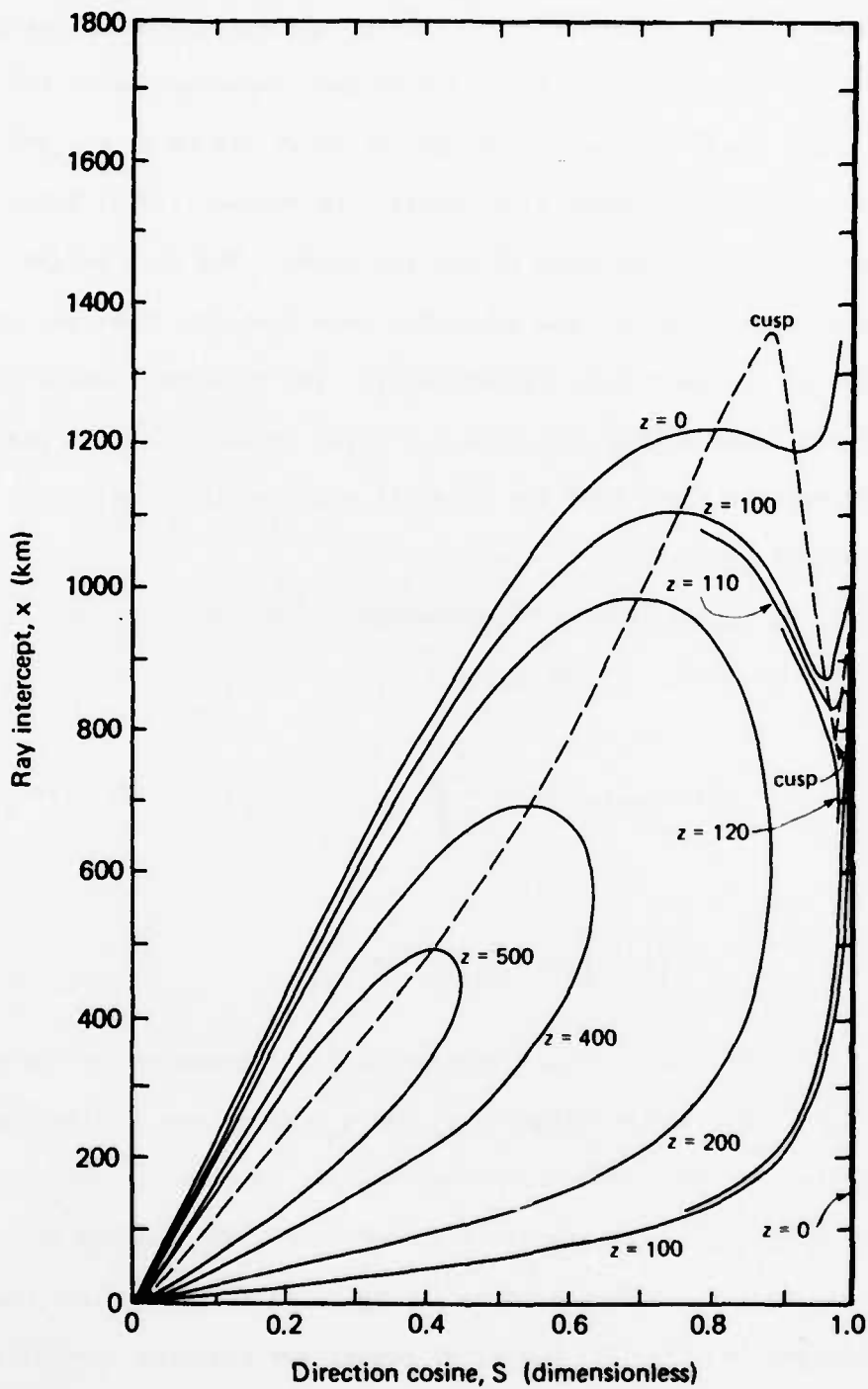


Fig. 1--Ray intercepts on horizontal planes at various heights z for the linear ionospheric model (27), with $h = 100$ km, $\alpha = 0.002$ km⁻¹. Caustic loci are shown as dashed lines that meet at two cusps.

have been left incomplete for $z = 110$ and 120 km. Dashed lines plot the loci of the caustics. The loci meet at two cusps--one below the ground at $x \sim 1360$ km, the other at a height of about 115 km at $x \sim 800$ km. A comparison of our figure with Figure 3 of *Maslin* [1976a] helps to clarify the configuration of the ray paths. For each height z in our figure, the up- and downgoing rays form the lower and upper branches of a closed loop, respectively. The branches connect at the reflection value $S_c(z)$; rays with $S > S_c(z)$ do not reach the height z . The figure also shows that the caustics are associated only with the downgoing branches.

For the magnetic dipole represented by (6), only the $n = \pm 1$ terms contribute to (22). In the plane $y = 0$,

$$F(x, 0, z) = e^{i\pi/4} (2\pi/kx)^{1/2} G_0 \int_{-1}^1 dS S^{3/2} (Cq)^{-1/2} 2\pi^{1/2} \xi^{1/4} \text{Ai}(\xi) \\ \times \exp \left\{ -ik \left[Sx + \frac{1}{2} (\phi_d + \phi_u) \right] \right\}, \quad (29)$$

with ξ given by (25). Here F represents the y -component of the electric field. The phase integrals ϕ_d and ϕ_u can be found either analytically (in this case) or through the ray tracing procedure discussed in Sec. III. To compare with *Maslin's* [1976b] asymptotic calculation, we set $z = 0$, $k = 4\pi \text{ km}^{-1}$. Owing to the very large phase oscillations in (29), its numerical evaluation requires special care. Appendix B describes a numerical quadrature method developed independently by *Woodie* [1976] and *Barakat* [1976], the piecewise linear phase (PLP) algorithm. Although more standard methods such as

the fast Fourier transform (FFT) could be as efficient as the PLP algorithm, we have obtained consistently good results using the latter with highly oscillatory integrals. Its application here with 100 sub-intervals produced the result shown in Figure 2 for the modulus of the field. Our figure agrees closely with Figure 3 of *Maslin* [1976b], even in the vicinity of the caustics at 1189.6 and 1226.7 km.

HYPERBOLIC SECANT PROFILE WITH COLLISIONS

A well-known model of an ionospheric layer is the hyperbolic secant profile

$$n^2 = 1 - \frac{a^2}{1 - iZ} \operatorname{sech}^2 [\alpha(z - z_m)] , \quad (30)$$

where a , Z , α , z_m are constants. For $Z = 0$, the ray intercepts in the plane $y = 0$ are given by Eq. (32) of *Maslin* [1976a]:

$$x(S) = \frac{S}{C\alpha} \ln \left[\frac{\left\{ C^2 \cosh^2 (-\alpha z_m) - a^2 \right\}^{1/2} - C \sinh (-\alpha z_m)}{\pm \left\{ C^2 \cosh^2 [\alpha(z - z_m)] - a^2 \right\}^{1/2} - C \sinh [\alpha(z - z_m)]} \right] . \quad (31)$$

Figure 3 plots $x(S)$ for various z , using $a = 0.9$, $\alpha = 0.05 \text{ km}^{-1}$, $z_m = 100 \text{ km}$, and ignoring collisions ($Z = 0$). For this choice of the parameter a , rays having $S < S_p = 0.43$ penetrate the layer and are not reflected at any height. The interpretation of Figure 3 is similar to that of Figure 1; the caustics are shown as dashed lines meeting at a single cusp at $z \approx 91 \text{ km}$. Again, for graphical clarity, two of the upgoing branches have been left incomplete.

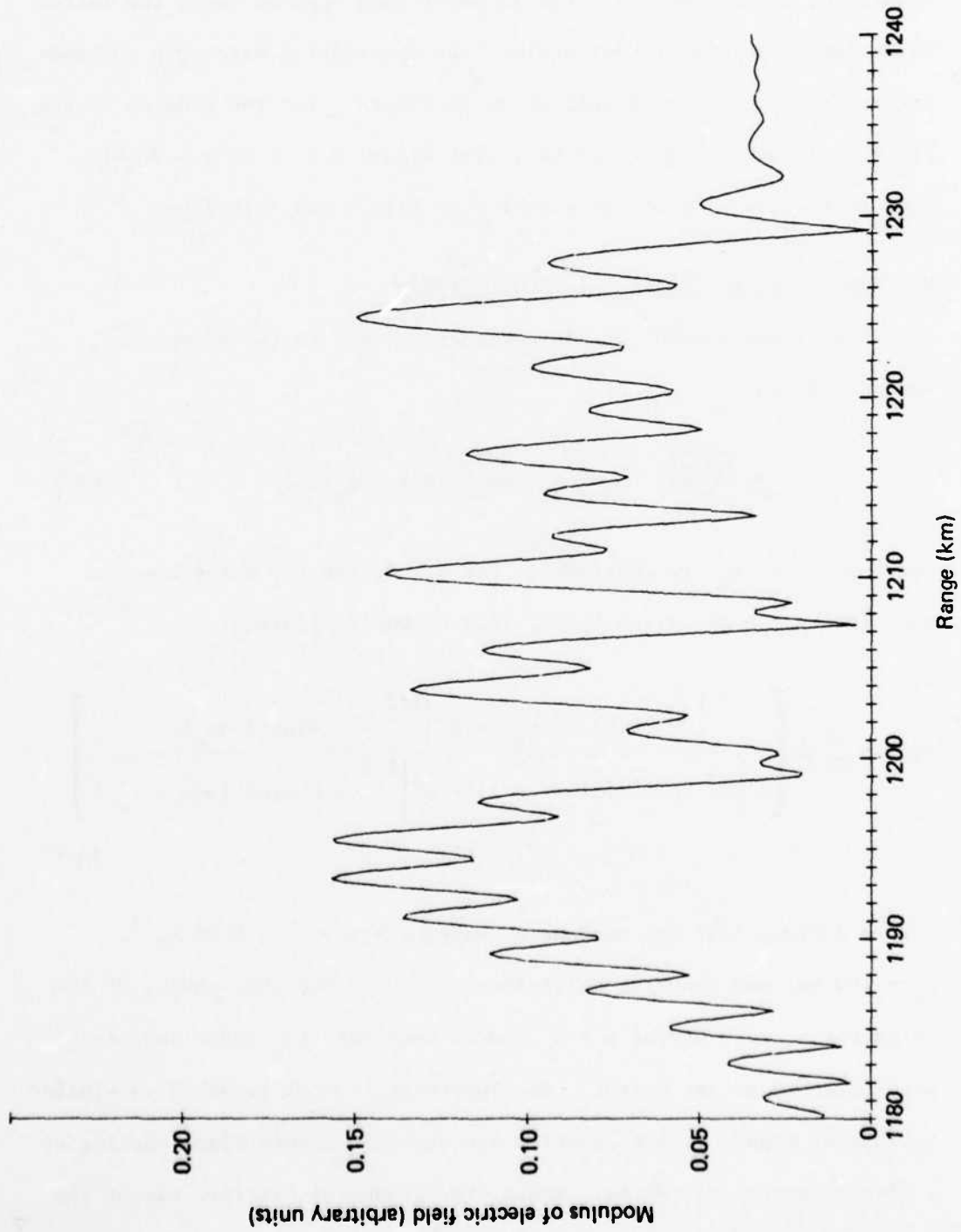


Fig. 2--Range dependence of the electric field modulus at the ground for the linear ionospheric model (27), with $h = 100$ km, $\alpha = 0.002$ km $^{-1}$.

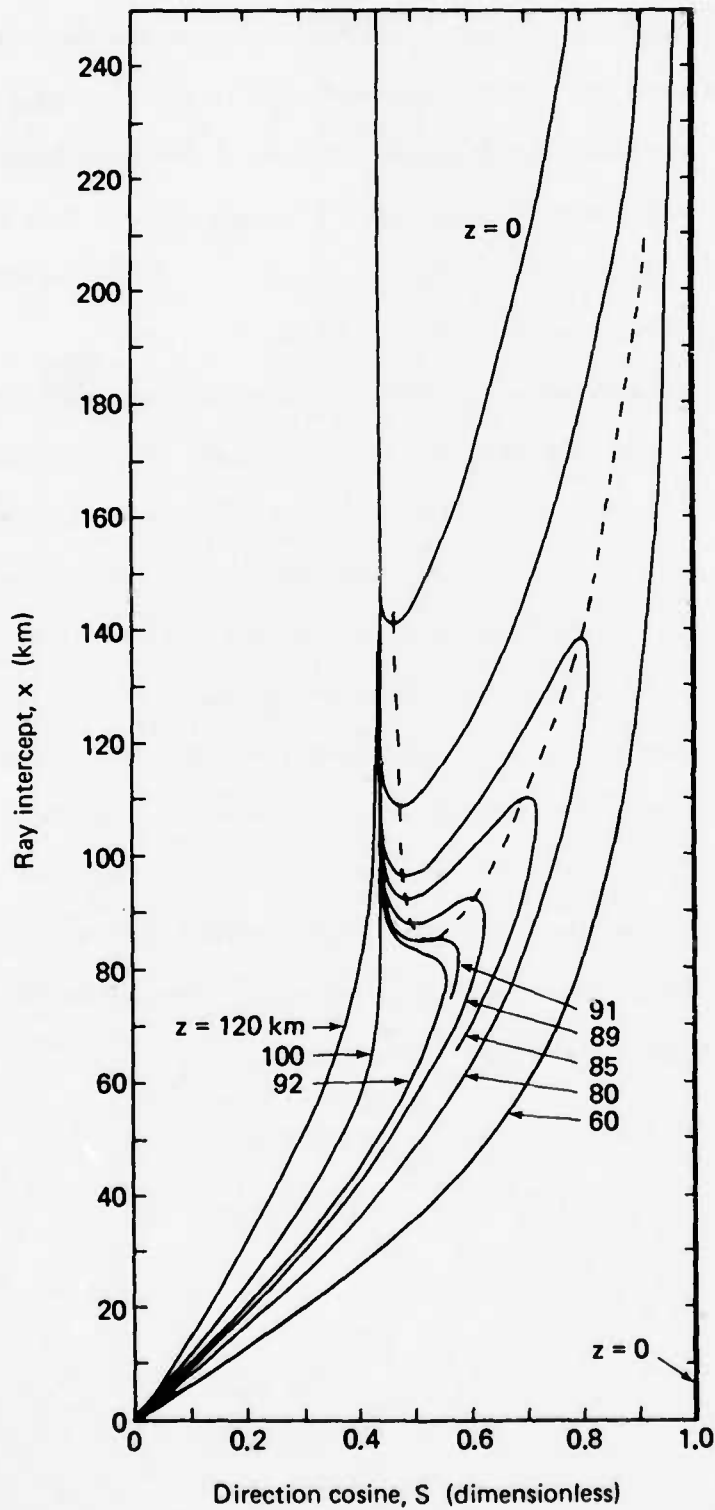


Fig. 3--Ray intercepts on horizontal planes at various heights z for the sech ionospheric model (30), with $a = 0.9$, $\alpha = 0.05 \text{ km}^{-1}$, $z_m = 100 \text{ km}$, $Z = 0$. Caustic loci are shown as dashed lines that meet at a single cusp at $z \approx 91 \text{ km}$.

To test the phase-integral estimation technique described in Sec. III, we used the *Jones/Stephenson* [1975] ray tracing program to compute ray intercepts $x(S)$ on the horizontal plane at height 88 km for both up- and downgoing rays with S values between 0.47 and 0.65. The fits were adjusted to yield $\phi_d = \phi_u$ for $S = 0.65$, corresponding to the ray grazing the plane at $z = 88$ km.

Collisions were modeled using the procedure suggested by *Booker* [1939] of propagating the rays as though they were real, but modifying the spectral weighting function G by the path-integrated attenuation for each ray traced. This was easily done, since the *Jones/Stephenson* program can compute the attenuation. For comparison with *Maslin* [1976b], constant collisions given by the parameter Z of 0, 0.0005, 0.0018, and 0.0045 were used. Application of the PLP algorithm to the magnetic dipole in the plane $y = 0$ produced the curves shown in Figure 4 for the modulus of the y -component of the field as a function of range. Our figure agrees well with Figure 6 of *Maslin* [1976b]. The two figures show the same reduction in oscillations for larger collision frequencies.

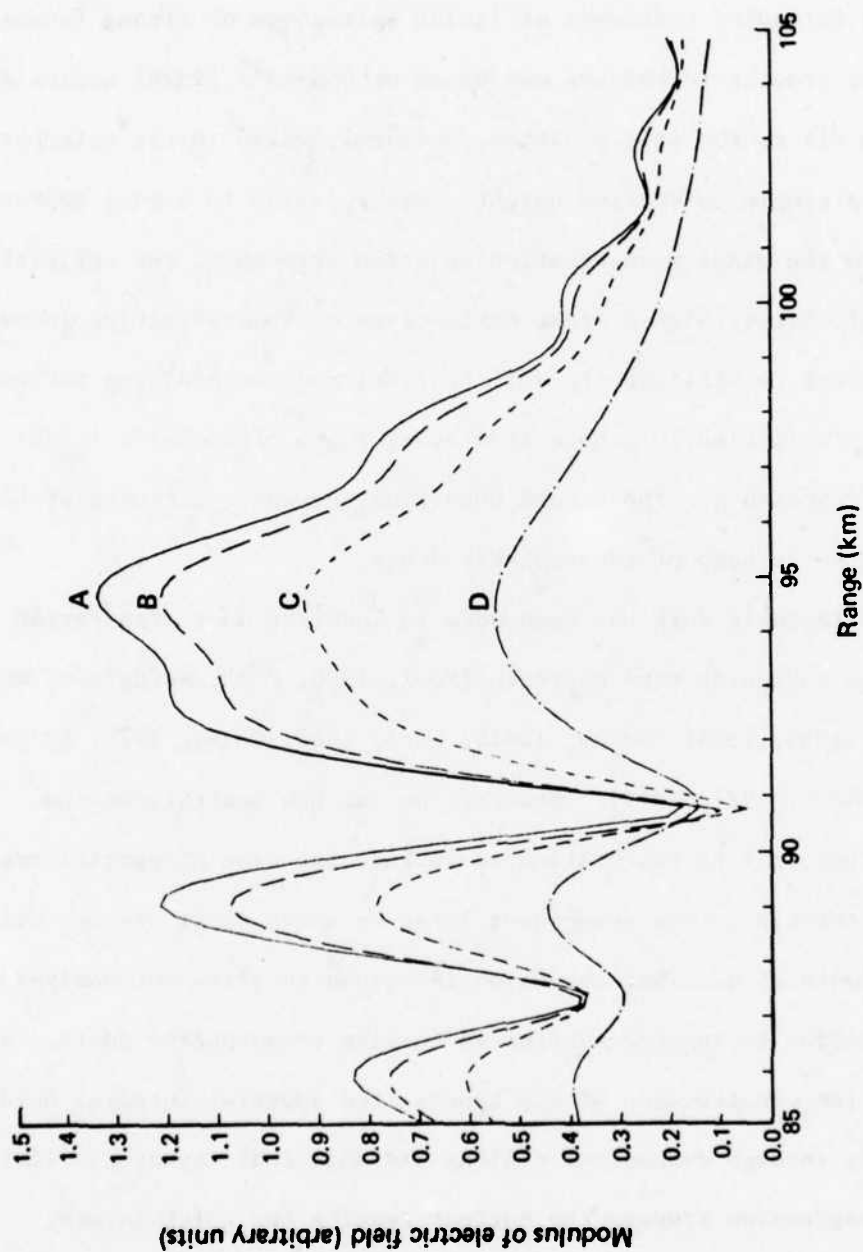


Fig. 4--Range dependence of the electric field modulus at a height z of 88 km for the linear ionospheric model $n^2 = 1 - a^2 \operatorname{sech}^2 [\alpha(z - z_m)]$, with $a = 0.9$, $\alpha = 0.05 \text{ km}^{-1}$, $z_m = 100 \text{ km}$. The different curves represent constant collision frequencies specified by the parameter Z :
A, 0; B, 0.0005; C, 0.0018; D, 0.0045.

V. UNIFORM ANGULAR SPECTRAL REPRESENTATION FOR AN EVANESCENT LAYER

The foregoing treatment of fields in regions of strong focusing using ray tracing techniques was based on *Budden's* [1976] approximate solution (1) to the wave equation, uniformly valid in the neighborhood of a single reflection height. His solution is a good approximation to the exact wave-equation solution throughout the reflection region if, first, higher order derivatives of the refractive index with respect to altitude are well behaved; and, second, the reflection height is sufficiently remote from other roots of *Booker's* [1939] quartic function q . The second condition, however, excludes problems such as the leakage of tropospheric ducts.

Considerable work has been done in modeling duct propagation using the waveguide mode approach [*Fock*, 1950; *Fock, Weinstein, and Belkina*, 1956, 1958; *Budden*, 1961b; *Wait*, 1962; *Chang*, 1971; *Pappert and Goodhart*, 1977, 1979]. However, no one has generalized the angular spectral representation to include the case of partial transmission through a thin evanescent layer in which there are two neighboring roots of q . That extension is needed to allow our analysis to be applied to superrefraction in leaking tropospheric ducts. We outline the construction of the generalized spectral integral holding uniformly through evanescent regions and show that asymptotic limits of the expression produce the correct results for thick layers.

It is well known that any field component F in free space can be written as a superposition of plane waves as

$$F(x, y, z) = \iint dS_1 dS_2 G(S_1, S_2) \exp \left[-ik(S_1 x + S_2 y + Cz) \right] . \quad (32)$$

In a medium varying in z only, the x - and y -dependence of a given spectral component of F in (32) is unchanged but the z -dependence is determined approximately by the equation

$$\frac{\partial^2 F}{\partial z^2} + k^2 q^2 F = 0 . \quad (33)$$

Additional terms involving derivatives of n may be present in (33), depending on the choice of transmitter and field component; they are neglected here. We wish to solve (33) approximately for the case in which there are two arbitrarily close roots $z_1 \leq z_2$ of q . For concreteness, we assume

$$\begin{aligned} q^2 > 0 , \quad z > z_2, z < z_1 , \\ q^2 < 0 , \quad z_1 < z < z_2 . \end{aligned} \quad (34)$$

This choice corresponds to the case of an evanescent region between $z_1 < z < z_2$ with real, propagating rays outside. The complementary problem of taking

$$\begin{aligned} q^2 > 0 , \quad z_1 < z < z_2 , \\ q^2 < 0 , \quad z > z_2, z > z_1 , \end{aligned} \quad (34a)$$

represents an elevated duct. Because the latter case has been well researched [Fock, Weinstein, and Belkina, 1956, 1958; Wait, 1962], we concentrate on the evanescent-layer problem.

For large k , (33) is a special case of a more general equation studied by *Langer* [1959]. The essence of his method is to change variables to produce an equation resembling *Weber's* [1869] equation asymptotically as $k \rightarrow \infty$. The change of variables is defined, first, by the equation

$$\int_{\xi}^{-1} dx(x^2 - 1)^{1/2} = \frac{\pi}{2Q} \int_z^{z_1} dzq, \quad (35)$$

with

$$Q \equiv \int_{z_1}^{z_2} dz|q|; \quad (36)$$

and, second, by

$$F(z) = \frac{(\xi^2 - 1)^{1/4}}{q^{1/2}} u(\xi), \quad (37)$$

in terms of which (33) becomes

$$\frac{d^2 u}{d\xi^2} + \left[\left(\frac{2kQ}{\pi} \right)^2 (\xi^2 - 1) - \frac{3}{4} \left(\frac{z''}{z'} \right)^2 + \frac{1}{2} \frac{z'''}{z'} \right] u = 0. \quad (38)$$

Here

$$z' \equiv \frac{dz}{d\xi} = \frac{(\xi^2 - 1)^{1/2}}{q} \frac{2Q}{\pi}, \quad (39)$$

with analogous expressions for z'' and z''' . Following *Langer*, the arguments of q and $(\xi^2 - 1)^{1/2}$ in (35) are defined as

$$\arg q(z) = \arg (\xi^2 - 1)^{1/2} = \begin{cases} 0, & z < z_1 \text{ and } \xi < -1, \\ \pi/2, & z_1 < z < z_2 \text{ and } -1 < \xi < 1, \\ 0, & z > z_2 \text{ and } \xi > 1. \end{cases} \quad (40)$$

Equation (35) thus can be used to define a mapping between heights throughout the region of the layer and the real line. For sufficiently high frequencies, the last two terms in (38) are small relative to the first two; dropping them and using the substitution

$$t \equiv 2 \left(\frac{kQ}{\pi} \right)^{1/2} \xi, \quad W(t) = u(\xi), \quad (41)$$

produces the following form of *Weber's* equation:

$$\frac{d^2 W}{dt^2} + \left(\frac{t^2}{4} - \frac{kQ}{\pi} \right) W = 0. \quad (42)$$

Besides *Weber* [1869], many others have studied solutions to this equation, including *Darwin* [1949], *Miller* [1952], *Olver* [1959], and *Erdélyi, Kennedy, and McGregor* [1954]. *Abramowitz and Stegun* [1965] summarize those previous analyses. Using the normalization and notation in *Abramowitz and Stegun*, two independent solutions of (42) are given by

$$W \left(\frac{kQ}{\pi}, \pm t \right).$$

Physical requirements dictate the proper combination of these solutions. For $kQ/\pi \gg 1$, we require the result to agree with *Budden's* [1976] uniform asymptotic result for z near z_1 . For $z \gg z_2$, the

solution should represent an outgoing plane wave. As shown below, those limits can be achieved by choosing the combination

$$E^* \left(\frac{kQ}{\pi}, t \right) \equiv \mu^{-1/2} W \left(\frac{kQ}{\pi}, t \right) - i\mu^{1/2} W \left(\frac{kQ}{\pi}, -t \right), \quad (43)$$

with

$$\mu \equiv \left(1 + e^{2kQ} \right)^{1/2} - e^{kQ}. \quad (44)$$

From (37), (41), and (43), the expression for a single spectral component is

$$F = A \frac{(\xi^2 - 1)^{1/4}}{q^{1/2}} E^* \left(\frac{kQ}{\pi}, 2\sqrt{\frac{kQ}{\pi}} \xi \right). \quad (45)$$

The factor A is chosen to match *Budden's* result for $z \ll z_1$ when kQ/π is large:

$$A = e^{i\pi/4} C^{1/2} \left(\frac{kQ}{\pi} \right)^{1/4} e^{-kQ} \left(1 - \frac{1}{4} e^{-2kQ} \right) \exp \left(-ik \int_0^{z_1} dzq \right). \quad (46)$$

Finally, the complete expression for F is

$$\begin{aligned} F = & \iint dS_1 dS_2 G(S_1, S_2) (C/q)^{1/2} e^{i\pi/4} \left(\frac{kQ}{\pi} \right)^{1/4} (\xi^2 - 1)^{1/4} \\ & \times e^{-kQ} \left(1 - \frac{1}{4} e^{-2kQ} \right) \exp \left(-ik \int_0^{z_1} dzq \right) E^* \left(\frac{kQ}{\pi}, 2\sqrt{\frac{kQ}{\pi}} \xi \right) \\ & \times \exp \left[-ik(S_1 x + S_2 y) \right]. \end{aligned} \quad (47)$$

This is the desired generalization, holding uniformly throughout an attenuating layer, of *Budden's* result for a single reflection level.

ASYMPTOTIC LIMITS

The expression (47) must be shown to produce the correct asymptotic limits for a thick evanescent layer. For kQ/π large, we apply the asymptotic approximations in terms of Airy functions given by *Abramowitz and Stegun* [1965]:

$$W\left(\frac{kQ}{\pi}, 2\sqrt{\frac{kQ}{\pi}}\xi\right) \approx 2\pi^{1/2} \left(\frac{4kQ}{\pi}\right)^{-1/4} \exp\left(\frac{1}{2}kQ\right) \left(\frac{\zeta}{\xi^2 - 1}\right)^{1/4} \text{Ai}(-\zeta) \quad (48)$$

and

$$W\left(\frac{kQ}{\pi}, -2\sqrt{\frac{kQ}{\pi}}\xi\right) \approx \pi^{1/2} \left(\frac{4kQ}{\pi}\right)^{-1/4} \exp\left(-\frac{1}{2}kQ\right) \left(\frac{\zeta}{\xi^2 - 1}\right)^{1/4} \text{Bi}(-\zeta), \quad (49)$$

where

$$\zeta \equiv \left(\frac{3kQ}{\pi} \int_{\xi}^{-1} dx(x^2 - 1)^{1/2}\right)^{2/3}, \quad \xi \leq -1, \quad (50)$$

$$\equiv -\left(\frac{3kQ}{\pi} \int_{-1}^{\xi} dx(1 - x^2)^{1/2}\right)^{2/3}, \quad \xi \geq -1, \quad (51)$$

and $\xi \leq 0$. Using (35) gives

$$\zeta = \left(\frac{3}{2}k \int_z^{z_1} dzq\right)^{2/3}, \quad z < z_1, \quad (52)$$

$$= -\left(\frac{3}{2}k \int_{z_1}^z dz|q|\right)^{2/3}, \quad z_1 < z < z_2. \quad (53)$$

From (44),

$$\mu \approx \frac{1}{2} e^{-kQ} . \quad (54)$$

Combining (43), (48), (49), and (54) gives

$$E^* \left(\frac{kQ}{\pi} , 2\sqrt{\frac{kQ}{\pi}} \xi \right) \approx (2\pi)^{1/2} \left(\frac{4kQ}{\pi} \right)^{-1/4} \left(\frac{\zeta}{\xi^2 - 1} \right)^{1/4} \\ \times \left[2 e^{kQ} \text{Ai}(-\zeta) - i \frac{1}{2} e^{-kQ} \text{Bi}(-\zeta) \right] . \quad (55)$$

For $z \ll z_1$, the Airy functions can be replaced by their asymptotic approximations:

$$\text{Ai}(-\zeta) \approx \pi^{-1/2} \zeta^{-1/4} \sin \left(k \int_z^{z_1} dzq + \frac{\pi}{4} \right) \quad (56)$$

and

$$\text{Bi}(-\zeta) \approx \pi^{-1/2} \zeta^{-1/4} \cos \left(k \int_z^{z_1} dzq + \frac{\pi}{4} \right) . \quad (57)$$

Expanding the trigonometric functions in their exponential representations, substituting into (55), and collecting terms, we obtain

$$E^* \left(\frac{kQ}{\pi} , 2\sqrt{\frac{kQ}{\pi}} \xi \right) \approx \left(\frac{kQ}{\pi} \right)^{-1/4} (\xi^2 - 1)^{-1/4} \exp \left(-i \frac{\pi}{4} \right) e^{kQ} \left(1 + \frac{e^{-2kQ}}{4} \right) \\ \times \exp \left(ik \int_0^{z_1} dzq \right) \left[\exp \left(-ik \int_0^z dzq \right) \right. \\ \left. + i \exp \left(-i2k \int_0^{z_1} dzq \right) \left(1 - \frac{e^{-2kQ}}{2} \right) \exp \left(ik \int_0^z dzq \right) \right] . \quad (58)$$

Substituting (58) and (46) into (45) gives

$$F \approx (C/q)^{1/2} \left[\exp \left(-ik \int_0^z dzq \right) + i \exp \left(-i2k \int_0^{z_1} dzq \right) \right. \\ \left. \times \left(1 - \frac{e^{-2kQ}}{2} \right) \exp \left(ik \int_0^z dzq \right) \right], \quad z \ll z_1. \quad (59)$$

This represents the usual decomposition of the field far below the layer into upgoing and downgoing waves with reflection coefficient

$$R = i \exp \left(-i2k \int_0^{z_1} dzq \right) \left(1 - \frac{e^{-2kQ}}{2} \right), \quad (60)$$

which in turn yields

$$|R|^2 \approx 1 - e^{-2kQ} \approx \frac{1}{1 + e^{-2kQ}} \quad (61)$$

to terms of second order in e^{-kQ} . The last result is a generalization of the reflection coefficient expression for a parabolic layer [Budden, 1961a].

For z near the higher root z_2 of q , applying (48) and (49) to (43) gives

$$F \approx \exp \left(i \frac{\pi}{4} \right) (C/q)^{1/2} \pi^{1/2} e^{-kQ} \exp \left(-ik \int_0^{z_1} dzq \right) \\ \times \zeta^{1/4} [Bi(-\zeta) - iAi(-\zeta)], \quad (62)$$

where

$$\zeta = - \left(\frac{3}{2} k \int_z^{z_2} dz |q| \right)^{2/3}, \quad z_1 < z < z_2, \quad (63)$$

$$= \left(\frac{3}{2} k \int_{z_2}^z dz q \right)^{2/3}, \quad z > z_2. \quad (64)$$

For $z \gg z_2$, the Airy functions can be approximated as

$$\text{Ai}(-\zeta) \approx \pi^{-1/2} \zeta^{-1/4} \sin \left(k \int_{z_2}^z dz q + \frac{\pi}{4} \right) \quad (65)$$

and

$$\text{Bi}(-\zeta) \approx \pi^{-1/2} \zeta^{-1/4} \cos \left(k \int_{z_2}^z dz q + \frac{\pi}{4} \right). \quad (66)$$

Substituting into (62) produces the field far above the layer

$$F \approx (C/q)^{1/2} \exp \left(-ik \int_0^{z_1} dz q \right) e^{-kQ} \exp \left(-ik \int_{z_2}^z dz q \right), \quad (67)$$

which is seen to be an outgoing plane wave, as required.

NUMERICAL EXAMPLE

The energy transmission through an evanescent layer is given approximately by (61) or (67) as

$$|T|^2 \approx e^{-2kQ}. \quad (68)$$

For the hyperbolic secant layer used in Sec. IV (with $Z = 0$), (36) gives

$$Q = 2 \frac{a}{\alpha} \int_0^{\cosh^{-1} a/C} du \left(\operatorname{sech}^2 u - C^2/a^2 \right)^{1/2}, \quad C \leq C_p,$$

$$= 0, \quad C > C_p, \quad (69)$$

where $C_p = a$. Rays with $C > C_p$ (or $S < S_p$) are refracted but not attenuated by the layer. Following *Budden* [1961a], the parameter a represents f_p/f , where f and f_p are the wave and penetration frequencies, respectively. For

$$k \frac{a}{\alpha} = \frac{2\pi f_p}{c\alpha} \gg 1,$$

$a/C \approx 1$ and

$$Q \approx \pi \frac{a}{\alpha} \left(\frac{a}{C} - 1 \right). \quad (70)$$

Substituting into (68) gives

$$|T|^2 \approx \exp \left[-2\pi \frac{ka}{\alpha} \left(\frac{a}{C} - 1 \right) \right]. \quad (71)$$

Figure 5 plots $|T|^2$ versus S computed with (71) for $\alpha = 0.05 \text{ km}^{-1}$, $k = 4\pi \text{ km}^{-1}$, and various values of a .

As expected, $|T|^2$ falls rapidly with increasing S beyond S_p . Nevertheless, for frequencies close to the penetration frequency ($a \sim 1$), plane wave components within ~ 3 deg of vertical will suffer less than 10 dB loss and should be included in the spectral integral (47).

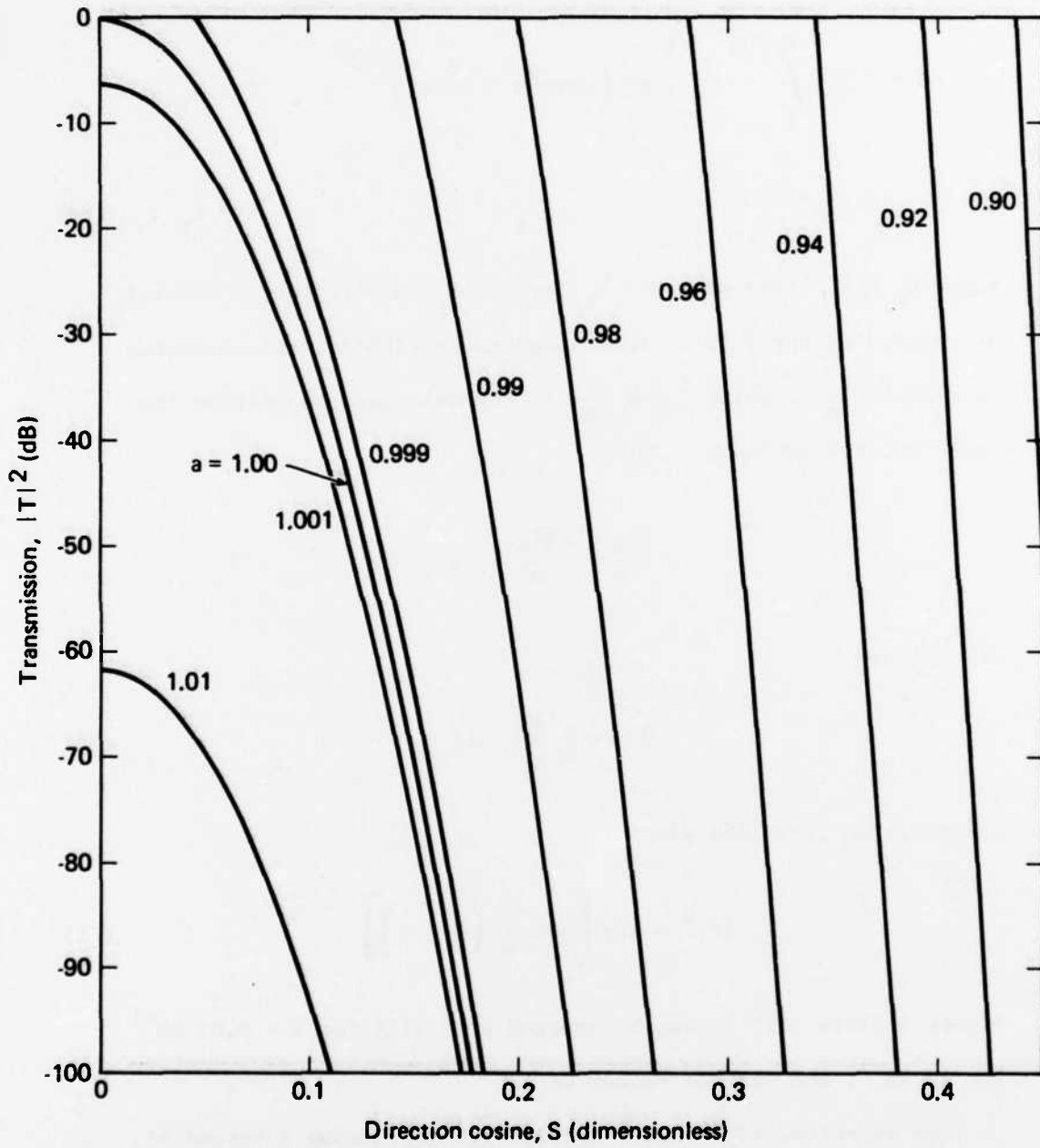


Fig. 5--Transmission through the sech ionospheric layer, Eq. (30), at various values of the parameter $a = f/f_0$

VI. CONCLUSIONS

The numerical method presented here for modeling radio field strengths in caustic and cusp regions has two advantages over the asymptotic method:

1. Use of a ray tracing program permits phase integrals for complicated media to be computed straightforwardly.
2. Use of numerical quadrature for spectral integration obviates the problems of locating and calculating the contributions of the stationary components in the integral, particularly when higher order asymptotic methods are necessary.

Numerical integration is both feasible and much easier even for the simple cases discussed here. Our algorithm avoids the excessive computer running time often associated with highly oscillatory integrands. For simple profiles amenable to asymptotic calculation, our method yields results nearly identical to those of *Maslin* [1976b]; moreover, it is applicable to a much broader range of profiles. Weak collisions can be included through use of attenuation information provided by the ray trace. Possible generalizations would include treatment of anisotropic media and leakage through thin layers. The latter problem is partially solved by extending the angular spectral integral to include regions throughout the vicinity of a thin layer.

REFERENCES

- Abramowitz, M., and I. Stegun (1965), *Handbook of Mathematical Functions*, 1046 pp., Dover, New York.
- Barakat, R. (1976), Sums of independent lognormally distributed random variables, *J. Opt. Soc. Am.*, 66, 211-216.
- Booker, H. G. (1939), Propagation of wave-packets incident obliquely upon a stratified doubly refracting ionosphere, *Philos. Trans. R. Soc. London*, 237, 411-451.
- Budden, K. G. (1961a), *Radio Waves in the Ionosphere*, 542 pp., Cambridge University Press, Cambridge, England.
- Budden, K. G. (1961b), *The Wave-Guide Mode Theory of Wave Propagation*, 325 pp., Prentice-Hall, Englewood Cliffs, N.J.
- Budden, K. G. (1976), Radio caustics and cusps in the ionosphere, *Proc. R. Soc. London, Ser. A*, 350, 143-164.
- Budden, K. G., and P. D. Terry (1971), Radio ray tracing in complex space, *Proc. R. Soc. London, Ser. A*, 321, 275-301.
- Chang, H. (1971), The waveguide mode theory of whispering-gallery propagation in the F region of the ionosphere, *Radio Sci.*, 6, 475-482.
- Chester, C., B. Friedman, and F. Ursell (1957), An extension of the method of steepest descents, *Proc. Cambridge Philos. Soc.*, 53, 599-611.
- Darwin, C. G. (1949), On Weber's function, *Quart. J. Mech. Appl. Math.*, 2, 311-320.
- Erdélyi, A., M. Kennedy, and J. L. McGregor (1954), Parabolic cylinder functions of large order, *J. Rat. Mech. Anal.*, 3, 459-485.

- Fock, V. A. (1950), Theory of radiowave propagation in an inhomogeneous atmosphere for a raised source, *Bull. Acad. Sci. USSR, Phys. Ser.*, 14, 70-94.
- Fock, V. A., L. A. Weinstein, and M. G. Belkina (1956), On radio wave propagation near the horizon with superrefraction, *Radio Eng. Electron. (USSR)*, 1, 575-592.
- Fock, V. A., L. A. Weinstein, and M. G. Belkina (1958), Radiowave propagation in surface tropospheric ducts, *Radio Eng. Electron. (USSR)*, 3, 1411-1429.
- Haselgrove, C. B., and J. Haselgrove (1960), Twisted ray paths in the ionosphere, *Proc. Phys. Soc. London*, 75, 357-363.
- Jones, R. M., and J. J. Stephenson (1975), *A Versatile Three-Dimensional Ray Tracing Computer Program for Radio Waves in the Ionosphere*, 185 pp., OT Report 75-76, U.S. Department of Commerce, Office of Telecommunications, Institute for Telecommunication Sciences, Boulder, Colo. 80302 (U.S. Government Printing Office, Washington, D.C. 20402).
- Langer, R. E. (1937), On the connection formulas and the solutions of the wave equation, *Phys. Rev.*, 51, 669-676.
- Langer, R. E. (1959), The asymptotic solutions of a linear differential equation of the second order with two turning points, *Trans. Am. Math. Soc.*, 90, 113-142.
- Maslin, N. M. (1976a), Caustics and cusps in an isotropic ionosphere, *J. Atmos. Terr. Phys.* 38, 239-250.
- Maslin, N. M. (1976b), Fields near a caustic and cusp in an isotropic ionosphere, *J. Atmos. Terr. Phys.*, 38, 1251-1263.
- Miller, J.C.P. (1952), On the choice of standard solutions of Weber's equation, *Proc. Cambridge Philos. Soc.*, 48, 428-435.

- Olver, F.W.J. (1959), Uniform asymptotic expansions for Weber parabolic cylinder functions of large order, *J. Res. Nat. Bur. Stand., Sec. B*, 63B, 131-169.
- Pappert, R. A., and C. L. Goodhart (1977), Case studies of beyond-the-horizon propagation in tropospheric ducting environments, *Radio Sci.*, 12, 75-87.
- Pappert, R. A., and C. L. Goodhart (1979), A numerical study of tropospheric ducting at HF, *Radio Sci.*, 14, 803-813.
- Pearcey, T. (1946), The structure of the electromagnetic field in the neighborhood of a cusp of a caustic, *Philos. Mag.*, 37, 311-317.
- Scheid, F. (1968), *Numerical Analysis, Schaum's Outline Series*, 422 pp., McGraw-Hill, New York.
- Wait, J. R. (1962), *Electromagnetic Waves in Stratified Media*, 372 pp., Pergamon, New York.
- Weber, H. F. (1869), Über die Integration der Parteilien Differentialgleichung: $\partial^2 u / \partial x^2 + \partial^2 u / \partial y^2 + k^2 u = 0$, *Math. Ann.*, 1, 1-36.
- Wong, M. S. (1958), Refraction anomalies in airborne propagation, *Proc. IRE*, 46, 1628-1638.
- Woodie, L. (1976), Two algorithms for numerical integration of the Huygens-Fresnel integral, in *Data Base Utilization, Phase I*, by A. R. Shapiro et al., PSR Report 509, Appendix A, pp. 93-100, Pacific-Sierra Research Corporation, 1456 Cloverfield Blvd., Santa Monica, Calif. 90404.

Appendix A

CURVE FITTING THE RAY INTERCEPT DATA

This appendix considers the problem of constructing phase integrals from ray trace intercept data on a plane at height z . Because of the polar symmetry in S , it is sufficient to consider rays in the plane $y = 0$. The up- and downgoing phase integrals $\phi_u(S, z)$ and $\phi_d(S, z)$ defined by (17) and (18), respectively, are found from rays penetrating the plane z from below or above. Using (16), one can find ϕ_u or ϕ_d up to constants by integrating an analytic representation of the ray intercepts $x(S)$ with respect to S . The problem then is one of curve fitting the ray data to a suitable set of basis functions over the range of S values that produce rays intersecting the plane. For the upgoing rays, that range extends from zero to the value S_c for which the ray is tangent to the plane. The downgoing range runs up to S_c from S_p , which labels the smallest incidence angle ray not penetrating the medium.

For a given height z , we require a fit to both branches of $x(S)$ for $S_0 \leq S \leq S_1$, where $S_1 < S_c(z)$. On the upgoing branch, $S_0 \geq 0$; on the downgoing branch, $S_0 > S_p$. The values of S_0 and S_1 must be chosen to include all rays near the x values for which the field is to be computed. Because of the well-known problem of numerical instability in least-squares fitting of a polynomial of degree greater than about five, orthogonal polynomials are often used as basis functions. A particularly convenient choice is the Chebyshev polynomial set, because of its orthogonality with respect to summations in

addition to its ability to produce a uniform fit over the function domain. Those properties are well described by *Scheid* [1968]. To use the orthogonality property, rays must be traced at definite, discrete values of S given by the equation

$$S_i = S_0 + (S_1 - S_0) \frac{(\rho_i + 1)}{2}, \quad i = 0, \dots, N - 1, \quad (\text{A.1})$$

where

$$\rho_i = \cos \left[(2i + 1) \frac{\pi}{2N} \right], \quad i = 0, \dots, N - 1, \quad (\text{A.2})$$

and N is the number of rays traced between S_0 and S_1 . Following *Scheid*, we approximate $x(S)$ with

$$x(S) \approx \sum_{k=0}^m \alpha_k T_k[\rho(S)], \quad m \leq N - 1, \quad (\text{A.3})$$

where T_k is the k th Chebyshev polynomial,

$$\rho(S) = \frac{2(S - S_0)}{S_1 - S_0} - 1, \quad (\text{A.4})$$

and the coefficients α_k are given by

$$\alpha_0 = \frac{1}{N} \sum_{i=0}^{N-1} x(S_i) \quad (\text{A.5})$$

and

$$\alpha_k = \frac{2}{N} \sum_{i=0}^{N-1} x(S_i) T_k(\rho_i), \quad 1 \leq k \leq m. \quad (\text{A.6})$$

For $m = N - 1$, this procedure produces a collocation polynomial through the data points $x(S_i)$; for smaller m , it yields a least-squares fit. Because of the orthogonality for a given N , the coefficients α_k are fixed for all fits of order $m \leq N - 1$. Therefore, in contrast to the usual least-squares polynomial fit, increasing the order of the approximation does not result in a reshuffling of lower order coefficients.

We illustrate the curve-fitting procedure using data produced from the *Jones/Stephenson* [1975] ray tracing program for the sech ionospheric model (30) with the parameters in Sec. IV and $z = 89$ km. We consider here only the downgoing rays and set $S_0 = 0.47$, $S_1 = 0.63$, $N = 12$. The table lists the coefficients produced for each fit with $0 \leq m \leq 11$ and the associated RMS defined as

$$\text{RMS} = \left\{ \frac{1}{N} \sum_{i=0}^{N-1} \left[x(S_i) - \sum_{k=0}^m \alpha_k T_k(\rho_i) \right]^2 \right\}^{1/2}. \quad (\text{A.7})$$

Only the highest degree α_m is given, because the α_k , $k < m$, are already determined. The RMS is given in kilometers, so a fifth-order fit produces a representation of the ray intercepts valid to about 0.03 km. The method thus should be accurate enough to produce reliable results in the angular spectral integration when used with *Maslin's* frequency of 600 kHz.

COEFFICIENTS PRODUCED BY CHEBYSHEV FITS
TO RAY TRACE INTERCEPT DATA

Order of Fit, m	Highest Degree Coefficient, α_m	RMS (km)
0	91.143250	1.8698
1	-2.358955	0.8448
2	0.771790	0.6449
3	0.901365	0.0983
4	0.027617	0.0963
5	0.128946	0.0311
6	-0.031670	0.0218
7	0.015146	0.0190
8	-0.002624	0.0189
9	0.013373	0.0165
10	-0.016300	0.0143
11	-0.019619	0.0029

Appendix B

PLP ALGORITHM

This appendix describes the numerical quadrature algorithm of *Woodie* [1976] and *Barakat* [1976] used in performing the plane-wave angular spectral integrations. The spectral integrals are of the form

$$I(x) = \int_{S_{\min}}^{S_{\max}} dS g(S) e^{-ikP(S,x)}, \quad (B.1)$$

where both $g(S)$ and $P(S, x)$ are continuous functions over the interval $S_{\min} < S < S_{\max}$. Because k can be large, the integrand contains a highly oscillatory phase term. Since $P(S, x)$ is continuous, we can subdivide the integration interval into N segments such that in the i th segment

$$P(S, x) \approx P(S_i, x) + \left. \frac{\partial P}{\partial S} \right|_{S_i} (S - S_i), \quad (B.2)$$

where $S_i = S_{\min} + \Delta S(i - 1/2)$, $i = 1, N + 1$, and $\Delta S = (S_{\max} - S_{\min})/N$. It is also assumed that N is large enough that $g(S) \approx g(S_i)$ within each element. Substituting into (B.1) produces

$$\begin{aligned} I(x) &\approx \sum_{i=1}^{N+1} g(S_i) e^{-ikP(S_i,x)} \int_{S_i-\Delta S/2}^{S_i+\Delta S/2} dS e^{-ikG(S_i,x)(S-S_i)} \\ &= \Delta S \sum_{i=1}^{N+1} g(S_i) e^{-ikP(S_i,x)} \frac{\sin kG(S_i,x) \Delta S/2}{kG(S_i,x) \Delta S/2}, \end{aligned} \quad (B.3)$$

where $G(S_i, x) = \left. \frac{\partial p}{\partial S} \right|_{S_i}$. Because of the approximation (B.2), this procedure has been named the piecewise linear phase (PLP) algorithm.

Its extension to two dimensions is straightforward.

SYMBOLS

$A(S, z)$ = Budden's reflection region factor, given by (4) or its asymptotic limit (5).

$Ai(\xi), Bi(\xi)$ = Airy integral functions.

C = z-direction cosine of plane wave component in free space.

$E^*(a, x)$ = parabolic cylinder function.

F = component of electromagnetic field.

$g_n(S)$ = n th azimuthal component of G .

$G(S_1, S_2)$ = spectral weighting function.

H = Hamiltonian.

J_n = n th Bessel function.

k = free-space wave number, ω/c , where ω is the angular frequency and c is the speed of light.

$n(z)$ = refractive index.

$q = [n^2(z) - S^2]^{1/2}$.

Q = integral of $|q|$ through the evanescent region.

$S = (S_1^2 + S_2^2)^{1/2}$.

S_1, S_2 = x- and y-direction cosines of plane wave component in free space.

$W(a, x)$ = Weber's function.

x, y, z = Cartesian coordinates with the z-axis vertically upwards.

$Z = \nu/\omega$, where ν is the electron collision frequency and ω is the angular frequency.

ξ = argument of Airy function given by (3).

$$\rho = (x^2 + y^2)^{1/2}.$$

τ = independent variable in Hamilton's ray equations.

$$\phi = \tan^{-1}(S_2/S_1).$$

$\phi_u(S_1, S_2, z)$ = phase integral for upgoing wave at height z .

$\phi_d(S_1, S_2, z)$ = phase integral for downgoing wave at height z .

$$\psi = \tan^{-1}(y/x).$$

A decorative border with a repeating floral or scrollwork pattern surrounds the central text.

MISSION
of
Rome Air Development Center

RADC plans and executes research, development, test and selected acquisition programs in support of Command, Control Communications and Intelligence (C³I) activities. Technical and engineering support within areas of technical competence is provided to ESD Program Offices (POs) and other ESD elements. The principal technical mission areas are communications, electromagnetic guidance and control, surveillance of ground and aerospace objects, intelligence data collection and handling, information system technology, ionospheric propagation, solid state sciences, microwave physics and electronic reliability, maintainability and compatibility.

ATE
LME

DTIC